

Effect of Ca^{2+} , Ba^{2+} , and Sr^{2+} on Alginate Microbeads

Yrr A. Mørch,^{*,§} Ivan Donati,[‡] Berit L. Strand,[§] and Gudmund Skjåk-Bræk[§]

Department of Biotechnology, Norwegian University of Science and Technology, Sem Sælands vei 6/8, 7491 Trondheim, Norway, and Department of Biochemistry, Biophysics and Macromolecular Chemistry, University of Trieste, Via Licio Giorgieri 1, 34127 Trieste, Italy

Received January 4, 2006; Revised Manuscript Received March 7, 2006

Microcapsules of alginate cross-linked with divalent ions are the most common system for cell immobilization. In this study, we wanted to characterize the effect of different alginates and cross-linking ions on important microcapsule properties. The dimensional stability and gel strength increased for high-G alginate gels when exchanging the traditional Ca^{2+} ions with Ba^{2+} . The use of Ba^{2+} decreased the size of alginate beads and reduced the permeability to immunoglobulin G. Strontium gave gels with characteristics lying between calcium and barium. Interestingly, high-M alginate showed an opposite behavior in combination with barium and strontium as these beads were larger than beads of calcium–alginate and tended to swell more, also resulting in increased permeability. Binding studies revealed that different block structures in the alginate bind the ions to a different extent. More specifically, Ca^{2+} was found to bind to G- and MG-blocks, Ba^{2+} to G- and M-blocks, and Sr^{2+} to G-blocks solely.

Introduction

Alginate microcapsules have for many years been used as immune barriers for cell transplantation where the alginate gel protects the transplant from the host immune system. Microencapsulation thus provides a potential way to overcome the need for immunosuppressive drugs. Although a variety of cells have been proposed and used for gel immobilization,^{1–3} major interest has been focused on employing alginate microcapsules for the encapsulation of Langerhans islets as a potential treatment for Type 1 diabetes. Alginate, the main component of these capsules, is a polysaccharide mainly isolated from brown algae. It is a linear copolymer consisting of guluronic (G) and mannuronic (M) acid forming regions of M-blocks, G-blocks, and of alternating structure (MG-blocks).⁴ Divalent cations such as calcium, barium, and strontium bind preferentially to the G-blocks in the alginate in a highly cooperative manner,⁵ thereby forming a gel. Alginate's affinity toward the different divalent ions has been shown to decrease in the following order: $\text{Pb} > \text{Cu} > \text{Cd} > \text{Ba} > \text{Sr} > \text{Ca} > \text{Co}, \text{Ni}, \text{Zn} > \text{Mn}$.^{6,7} Since the composition and block structure varies greatly in different types of alginates, it follows that both the gel and ion-binding properties of alginate is influenced by the choice of alginate material and cross-linking ion.

Traditionally, calcium has been used as the gel-forming ion in the production of gel beads for bioencapsulation purposes. However, Ca–alginate beads are sensitive toward chelating agents such as phosphate and citrate and nongelling agents such as sodium and magnesium ions. In physiological solution, this ion replacement results in osmotic swelling of the beads inevitably leading to increased pore size and destabilization and rupture of the gel.⁸ To increase the stability and reduce the permeability of Ca–alginate gel beads, a polycation layer is often added to the alginate gel core, following the original

microencapsulation protocol of Lim and Sun.⁹ Most polycations are, however, toxic to cells,¹⁰ and the most commonly used polycation for encapsulation purposes, poly-L-lysine (PLL), is the main capsule component responsible for the fibrotic overgrowth often seen on implanted alginate–PLL–alginate microcapsules.¹¹ Recently, much focus has therefore been on developing new methods omitting the polycation treatment, including the use of epimerized alginate¹² or covalently cross-linked alginate¹³ as core material.

Another method recently exploited by many groups giving promising results both in allo- and xenograft transplantation^{14–18} as well as in biocompatibility studies¹⁹ is the use of Ba–alginate instead of the traditional Ca–alginate. In principle, barium ions (Ba^{2+}) will, because of their higher affinity toward alginate, form stronger gels with alginate compared to calcium.²⁰ Nevertheless, the affinity is highly dependent on the alginate composition, and limited work has been done on characterizing the effect of different divalent ions on gel bead properties. Since barium is an inhibitor of K^+ channels in biomembranes at concentrations greater than 5–10 mM,²¹ the concentration should be kept at a minimum when used in vivo. Strontium, on the other hand, is a nontoxic divalent cation which has been scarcely tested for encapsulation purposes.

The aim of this study was to compare the effects of various gelling ions (Ca^{2+} , Ba^{2+} , and Sr^{2+}) on two alginates of different composition widely used for encapsulation purposes. We have studied the influence of Ca^{2+} , Sr^{2+} , and Ba^{2+} on microbead stability, permeability, and gel strength and on the distribution of alginate in gel beads. In addition, the binding of these divalent ions to both natural and enzymatically modified alginates of different composition was studied.

Materials and Methods

Alginates. High molecular weight sodium alginate samples isolated from *Macrocystis pyrifera* (high-M alginate) and *Laminaria hyperborea* stipes (high-G alginate) were provided by Sigma Chemicals (U.S.A.) and FMC Biopolymer (Norway), respectively. High molecular weight

* Corresponding author. Tel: (+47)73591689. Fax: (+47)73591283. E-mail: yrrm@ntnu.no.

§ Norwegian University of Science and Technology.

‡ University of Trieste.

Table 1. Chemical Composition and Sequences^a Obtained from ¹H NMR Spectra and Intrinsic Viscosity [η] for Alginates Used in the Present Study

source	F_G	F_M	F_{GG}	F_{MM}	$F_{MG/GM}$	$F_{GGM/MGG}$	F_{MGM}	F_{GGG}	$F_{G>1}$	[η] (mL/g) ^b
<i>M. pyrifera</i> (high-M)	0.40	0.60	0.21	0.40	0.20	0.05	0.18	0.16	5	823
<i>L. hyperborea</i> stipe (high-G)	0.66	0.34	0.55	0.22	0.12	0.05	0.09	0.50	13	619
PolyM	0	1	0	1	0	0	0	0	0	930
PolyG	0.93	0.07	0.88	0.05	0.03	0.02	0.01	0.86	>30	—
PolyMG	0.45	0.55	0	0.10	0.45	0	0.45	0	0	1566

^a F_G denotes the fraction of alginate consisting of guluronic acid. F_{GG} and F_{GGG} indicate the fraction of alginate consisting of guluronic acid in blocks of dimers and trimers, respectively, whereas F_{MM} indicates the fraction of alginate consisting of mannuronic diads. $F_{GGM/MGG}$ indicates the fraction of alginate which starts or ends with a block of guluronic acid. $F_{MG/GM}$ indicates the fraction of alginate consisting of mixed sequences of guluronic and mannuronic acid, with F_{MGM} denoting the fraction of alginate consisting of two mannuronic acids interspaced with guluronic acid. $N_{G>1}$ indicates the average length of guluronic acid blocks. ^b The intrinsic viscosity was measured at 20 °C in 0.1 M NaCl aqueous solution in a Micro Ubbelohde viscometer.

Table 2. Initial Size of Microbeads Made from Different Gelling Solutions^a

gelling solution	initial bead size after 10 min		initial bead size after 24 h	
	gelation (μ m)	std dev $n = 30$	gelation (μ m)	std dev $n = 30$
high-M alginate from <i>M. pyrifera</i>				
50 mM CaCl ₂	462	8	424	8
50 mM CaCl ₂ + 1 mM BaCl ₂	474	8	437	7
10 mM BaCl ₂	532	7	504	5
20 mM BaCl ₂	508	12	479	8
50 mM SrCl ₂	486	10	449	10
high-G alginate from <i>L. hyperborea</i> stipe				
50 mM CaCl ₂	510	5	480	6
50 mM CaCl ₂ + 1 mM BaCl ₂	519	8	485	6
10 mM BaCl ₂	516	6	484	8
20 mM BaCl ₂	490	11	464	20
50 mM SrCl ₂	496	18	467	16

^a All gelling solutions were in 0.15 M mannitol. The diameters are given as the mean of 30 beads.

mannuronan (polyM) was isolated from an epimerase-negative mutant (AlgG⁻) of *Pseudomonas fluorescens*.²² Polyalternating alginate (polyMG) was prepared from mannuronan using the epimerase AlgE4 obtained as reported elsewhere.²³ A low molecular weight ($M_w \sim 7200$) alginate fraction enriched in guluronic acid (polyG) was obtained by partial acid hydrolysis of *Laminaria digitata* alginate following the procedure by Haug et al.⁴ The chemical composition and intrinsic viscosity for the alginates are given in Table 1.

Formation of Microbeads. All beads were made by dripping a 1.8% (w/v) sterile filtered alginate solution (in 0.3 M mannitol, pH 7.4) into solutions containing divalent cations (CaCl₂, BaCl₂, and/or SrCl₂) with a concentration of 10–50 mM (in 0.15 M mannitol, pH 7.4 with 0.1% Tween20) using an electrostatic bead generator (7 kV, 10 mL/h, steel needle with outer diameter 0.4 mm, 1.7 cm distance from the needle to the gelling solution). This resulted in microbeads with an inhomogeneous alginate distribution and with diameters given in Table 2.

Stability Measurements and Size Determination. The dimensional stability of microbeads was measured as resistance against osmotic swelling in saline solution. Gel beads were made as described above and kept in gelling solution overnight. A total of 3 mL of saline solution was added to 0.5 mL of gel beads after removal of the gelling solution. The sample was kept on a turn-over stirrer for 1 h before the saline was removed and fresh solution added. The saline solution was exchanged six times. The size of beads was determined (using a Nikon Eclipse TS100 microscope and software SPOT version 3.5.2 and Matrox Inspector version 3.0) before each change of saline solution. Images were taken after 10 min and 24 h in gelling solution to determine the initial size of the beads.

Permeability of Radiolabeled IgG: Permeability of radiolabeled immunoglobulin G (IgG) into alginate gel beads was studied using encapsulated paramagnetic monosized polymer particles (Dynabeads M-450 Tosylactivated, Dynal, Norway) as described previously.²⁴ The Dynabeads were coupled with monoclonal mouse anti-human TNF antibodies as described by Liabakk et al.²⁵ The Dynabeads (4.5 μ m in diameter) were encapsulated into alginate beads by mixing a Dynabead suspension with Na–alginate to a final concentration of 0.4 mg Dynabeads/mL and 1.8% (w/v) alginate in 0.3 M mannitol. Alginate beads were made from a 2 mL alginate solution (three parallels) using the procedure as described above with varying gelling solutions. The alginate beads with encapsulated Dynabeads were washed 3 times in 3 mL of saline (30 s) and kept in 0.01 M Tris buffer (pH 7.4 at 25 °C), 0.9% (w/v) NaCl, 0.1% (w/v) bovine serum albumin (BSA), and 0.1% (w/v) Na–azide to a total of 1.9 mL before adding 100 μ L of [¹²⁵I]-labeled anti-mouse IgG from sheep (Amersham Biosciences, England). The radioactivity was approximately 30000 disintegrations per minute per tube. The mixture was kept on a turn-over stirrer for 20 h, the buffer was removed, and the capsules were washed 3 times in buffer containing 0.1% (w/v) Tween 20. The amount of radiolabeled IgG bound to encapsulated Dynabeads was measured in a γ counter (Cobra II Auto-Gamma, Packard). As a positive and negative control, nonencapsulated Dynabeads and empty capsules were used, respectively.

Permeability of Fluorescence-Labeled IgG: Permeability of fluorescence-labeled IgG into alginate microspheres was studied using encapsulated antibody-coated Dynabeads (Dynabeads M-450 Goat anti-Mouse IgG, Dynal, Norway). Mouse IgG (Sigma-Aldrich, U.S.A.) was fluorescence-labeled using Alexa Fluor 488 Protein Labeling Kit (Molecular Probes, U.S.A.). The concentration of Dynabeads was 1 mg/mL alginate solution. Alginate beads were made as described above using different gelling solutions. The beads were washed 3 times in saline before transferred to an assay buffer containing 0.01 M Tris (pH 7.4 at 25 °C), 0.9% (w/v) NaCl, 0.1% (w/v) bovine serum albumin (BSA), and 0.1% (w/v) Na–azide. A 4-well glass slide (Nalge Nunc International, U.S.A.) was covered with a monolayer of beads with 0.5 mL of the assay buffer, and 1.4 μ g of fluorescence-labeled IgG was added. The diffusion of fluorescence-labeled IgG was monitored with a Confocal Laser Scanning Microscope using a 488 nm Argon laser as described above. As a positive and negative control, free Dynabeads in solution and capsules without Dynabeads were used, respectively.

Alginate Distribution in the Gel. The high-G and high-M alginates were fluorescence-labeled with fluoresceinamine (C₂₀H₁₃NO₃, mixed isomers, Sigma) as previously described.²⁶ Briefly, the alginates were dissolved in PBS to give 90 mM carboxylic groups before EDC (Sigma) and Sulfo-NHS (Fluka) were added to 9 mM of each and kept for 2 h. Fluoresceinamine was added to a concentration of 0.036 mM (corresponding to labeling 1/2500 carboxylic groups), and the reaction mixture was kept for 18 h in the dark at room temperature. Unreacted fluoresceinamine was removed by dialysis overnight against ion-free water followed by three shifts in 1 M NaCl and finally against ion-free water (5 shifts). Alginate gel beads were made from 1.8% (w/v)

high-M and high-G alginate (in 0.3 M mannitol) gelled in barium, strontium, and/or calcium solutions (in 0.15 M mannitol). The alginate beads were visualized using a Zeiss LSM 510 confocal laser scanning microscope (CLSM) with a Plan-Neofluar 10 \times /0.3 objective and LSM 510 software, release 3.0 SP2 (Carl Zeiss, Germany). The settings for the confocal microscope and the imaging of beads were computer-controlled. All images were obtained by a mean of eight scans through an equatorial slice of the beads. For visualization of alginate, a 488 nm Argon laser was used and the fluorescence detected with a 500–550 nm bypass filter.

Gel Strength Measurements and Syneresis. Alginate gel cylinders were made by internal gelling using the CaCO₃/GDL method described in a previous paper²⁷ followed by dialysis against solutions of BaCl₂, SrCl₂, and/or CaCl₂ in 0.2 M NaCl. Briefly, solutions of high-M and high-G alginate were mixed with an inactivated form of Ca²⁺ (CaCO₃, average particular size 4 μ m, Merck, Germany) followed by the addition of the slowly hydrolyzing D-glucono- δ -lactone (GDL, Sigma Chemical, U.S.A.), maintaining a molar ratio [GDL]/[Ca²⁺] = 2. The final concentration of CaCO₃ and alginate was 15 mM and 1% (w/v), respectively. The gels were cured in 24-well tissue culture plates having a diameter of 16 mm and height of 18 mm (Costar, U.S.A.) for 24 h. The gel cylinders were then taken out of the wells and transferred to various solutions of barium, strontium, and calcium (all in 0.2 M NaCl) for saturation. The gels were kept in the gelling solutions for 48 h on a shaker at 4°C, changing the solution once.

Young's modulus (E) of the resulting gels was calculated from the initial slope of the force/deformation curve²⁰ as measured with a Stable Micro Systems TA-XT2 Texture analyzer at 22 \pm 1°C. The rate of compression was 0.1 mm/s. Syneresis of the gels was determined as the weight reduction of gel cylinders with respect to the initial weight, assuming a density value of 1. For all gels exhibiting syneresis, the final concentration was determined and E was corrected adapting $E \propto c^{2.28}$.

Circular Dichroism Spectroscopy. Circular dichroic spectra of the sodium form of high-M and high-G alginate and of polyM, polyG, and polyMG were recorded in deionized water ($c \sim 2 \times 10^{-3}$ monomol/L) with a Jasco J-700 spectropolarimeter. A quartz cell of 1 cm optical path length was used and the following setup maintained: bandwidth = 1 nm; time constant = 2 s; scan rate = 20 nm/min. Four spectra corrected for the background were averaged for each sample. The spectrum of each sample was recorded prior to and after the addition of Ca(ClO₄)₂, Ba(ClO₄)₂, or Sr(ClO₄)₂ with an increasing [ion²⁺]/[Polym_{in}] (R_j) ratio.

Results

Initial Size and Swelling of Alginate Beads. High-M and high-G alginate beads gelled in Ba²⁺, Sr²⁺, and/or Ca²⁺ solutions of different concentrations were compared with regard to initial size and swelling capacity in saline solution. As shown in Table 2, high-M Ca–alginate beads were smaller than corresponding beads of high-G alginate, which is in accordance with earlier observations.²⁹ However, the presence of barium and strontium seemed to increase the initial size of gel beads compared to calcium for high-M alginate beads. This was not the case for the high-G alginate. Table 2 further demonstrates that the initial size of the gel beads was reduced when the beads were kept in gelling solution overnight, allowing the alginate chains to make a more compact gel network.

In the body, alginate capsules are expected to swell due to the exchange of Ca²⁺ with Na⁺ leading to destabilization of the gel network.²⁸ The beads listed in Table 2 were therefore exposed to extreme conditions by placing them in saline solution free of divalent cations in order to monitor the osmotic swelling (Figure 1). Interestingly, alginate capsules of high-G and high-M alginate showed great differences in their stability toward swelling depending on the gelling ions used. For high-G alginate,

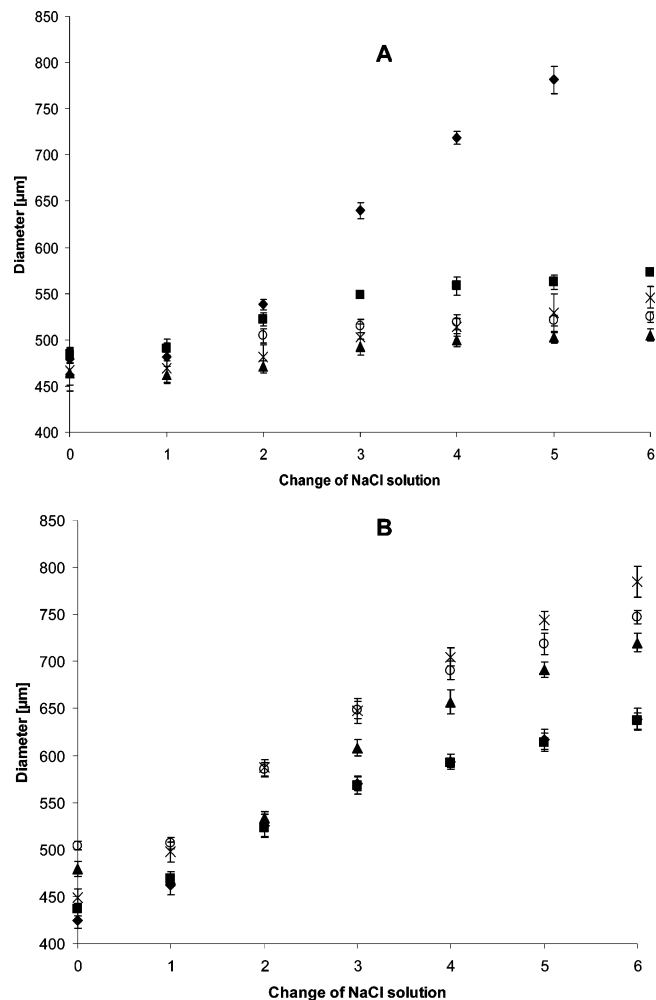


Figure 1. Swelling of alginate beads in 0.9% NaCl. The beads were gelled in various gelling solutions (all in 0.15 M mannitol): 50 mM CaCl₂ (◆), 50 mM CaCl₂ + 1 mM BaCl₂ (■), 10 mM BaCl₂ (○), 20 mM BaCl₂ (▲), 50 mM SrCl₂ (×). The saline solution was exchanged every hour and the diameter measured after each exchange. A: High-G alginate. B: High-M alginate. Capsule diameter is given as mean \pm SD of 30 beads.

the swelling was highly reduced when barium and strontium were used as cross-linking ions instead of the traditional calcium ions (Figure 1A). The addition of only 1 mM BaCl₂ to the CaCl₂ solution was enough to reduce the swelling by 28% compared to pure calcium beads at the fifth shift of saline solution. High-G alginate beads made in the presence of 20 mM Ba²⁺ were most stable, with an increase in diameter of only 8% after six shifts of saline.

For high-M alginate, however, no reduction on swelling was detectable upon exchanging Ca²⁺ with Sr²⁺ or Ba²⁺ (Figure 1B). In fact, strontium seemed to bind to a lesser extent to high-M alginate as compared to calcium, as seen from the high degree of swelling (75% increase in diameter) after six shifts of saline.

Permeability. Since barium–alginate beads without an outer polycation layer have given promising results both in allo- and xenograft transplantation,^{14–18} it was of special interest to study the permeability of different alginate beads toward immunoglobulin G (IgG). IgG is the smallest antibody (150 kD) and is generally considered important to keep out of alginate beads to prevent an immune reaction toward encapsulated cells.

The permeability of [¹²⁵I]-labeled IgG into beads of high-M and high-G alginate made in various gelling solutions is given

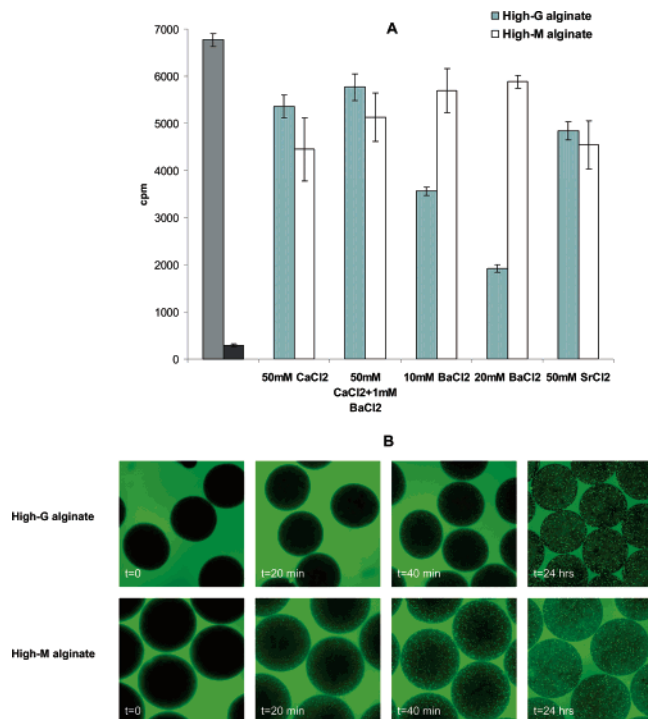


Figure 2. Permeability of high-G and high-M alginate beads to IgG. A: Permeability of [¹²⁵I]-labeled IgG into beads of high-G and high-M alginate gelled in various ionic solutions. Dark gray: Dynabeads in solution (positive control). Black: Empty beads (negative control). The radioactivity is measured in counts per minute (cpm). Results are given as mean \pm standard deviation of three parallels. B: Permeability of fluorescence-labeled IgG (green) into beads of high-G and high-M alginate gelled in 20 mM BaCl₂ at times $t = 0$, $t = 20$ min, $t = 40$ min, and $t = 24$ h after addition of IgG. Bead diameter is approx 500 and 630 μ m for high-G and high-M alginate, respectively.

in Figure 2A. The data show that barium in the gelling solution reduced the permeability of beads of high-G alginate drastically. Using 20 mM Ba²⁺ in the gelling solution decreased the amount of IgG in the beads from 79% of maximum penetration (for Ca-alginate beads) to 28%. For beads of high-M alginate on the other hand, addition of barium caused increased permeability, probably due to swelling of the beads. Strontium reduced the permeability somewhat in high-G alginate, whereas for high-M alginate the permeability seemed to increase slightly. Ca-alginate beads of high-M alginate were less porous than the corresponding spheres of high-G alginate. This is probably due to differences in size and swelling behavior for the two alginates (see Table 2).

Since beads of high-G alginate made with 20 mM BaCl₂ were rather impermeable to IgG (Figure 2), a question arose whether the IgG was associated with the surface or trapped in the outermost layer of these beads (where the alginate concentration is highest) or if the immunoglobulin was actually able to diffuse into the center of the beads. A method was therefore developed for visualizing bound IgG in the alginate beads using fluorescence-labeled IgG and encapsulated anti-mouse IgG coated Dynabeads.

Figure 2B shows CLSM images of Ba-alginate beads with encapsulated Dynabeads from high-M and high-G alginate gelled in 20 mM BaCl₂ after addition of fluorescence-labeled IgG (green). When IgG enters the beads, it will bind to the encapsulated Dynabeads which then will fluoresce. Although the diffusion of IgG was slower in beads of high-G alginate compared to high-M alginate, the figure illustrates that IgG had penetrated to the center of beads for both alginate types 24 h after addition of the antibody. Beads of Ca- and Sr-alginate

were also tested with regard to permeability of fluorescence-labeled IgG. Even though the diffusion rate of IgG varied for the different beads tested (data not shown), there were no *visual* differences with regard to IgG penetration 24 h after addition of the immunoglobulin.

Alginate Distribution in Gel Beads. Inhomogeneity has been explained as a result of a rapid and virtually irreversible gelling mechanism characterized by strong binding of the cross-linking ions. The steepness of the concentration gradient has been interpreted as stemming from the relative diffusion rate of the cross-linking ion and the polymer. Inhomogeneity is thus promoted by lowering the concentration of calcium ions in the gelling bath, while homogeneity is obtained by breaking the coupled diffusion of sodium alginate using a charged osmolyte such as NaCl.³⁰ Inhomogeneous Ca-, Ba-, and Sr-alginate beads from fluorescence-labeled high-M and high-G alginate were examined in the CLSM to see whether differences in the distribution of alginate in the gel could be observed. Images were obtained by scanning through a thin section of the capsule equator, and the intensity of the fluorescent light was measured. Figure 3 shows that for all beads examined, the concentration of alginate was higher at the bead surface than in the center. As there were no visual differences between beads of high-G and high-M alginate, only data on high-G alginate is given. Beads made in the presence of low concentrations of barium (10 mM BaCl₂) were showing the highest inhomogeneity with approximately five times higher concentration of alginate at the surface of the beads than in the center (Figure 3B). For Ca-alginate beads (50 mM Ca²⁺), the concentration difference was about 120%. This is in accordance with previous observations.^{26,31} Sr-alginate beads were similar to Ca-alginate beads. To see if the variations in alginate homogeneity were due to ion concentration differences rather than to differences in ion affinity, gel beads made in the presence of 20 mM Ca²⁺ were compared with beads of 20 mM Ba²⁺ and 50 mM Ca²⁺. Figure 3D illustrates that the beads of 20 mM Ca²⁺ were in fact more inhomogeneous than beads of 50 mM CaCl₂, showing that the concentration of ions in the gelling solution is of great importance when it comes to alginate distribution in the gel spheres.

Gel Strength. To compare the strength of alginate gels made of high-G and high-M alginate with various divalent ions, the elasticity modulus of alginate gel cylinders was studied by small deformation compression of the gels. Since alginate gel beads are dialysis gels, an attempt was made to produce homogeneous Ca-, Ba-, and/or Sr-alginate gel cylinders from 1.8% (w/v) alginate in 0.2 M NaCl by dialysis in various gelling solutions (all in 0.2 M NaCl) according to the method of Skjåk-Bræk et al.³⁰ Almost all the gel cylinders appeared to be inhomogeneous, showing a weaker area in the middle of the cylinder, making gel compression measurements difficult (data not shown). To overcome this problem, unsaturated Ca-alginate gel cylinders were made by internal gelling using calcium carbonate and the slowly hydrolyzing GDL. The gels were then transferred to different gelling solutions of Ba²⁺, Sr²⁺, and Ca²⁺ in 0.2 M NaCl in order to make saturated gels. The resulting gel cylinders did not show any sign of inhomogeneity, and compression of the gels gave very reproducible stress-strain curves.

In Figure 4 the gel strength (elasticity) of alginate cylinders is given as Young's modulus (E) for the different gels. High-G alginate gels were in all cases stronger than the corresponding gels of high-M alginate. For high-G alginate, even very low concentrations of barium increased the gel strength dramatically as addition of only 1 mM BaCl₂ in the gelling solution resulted

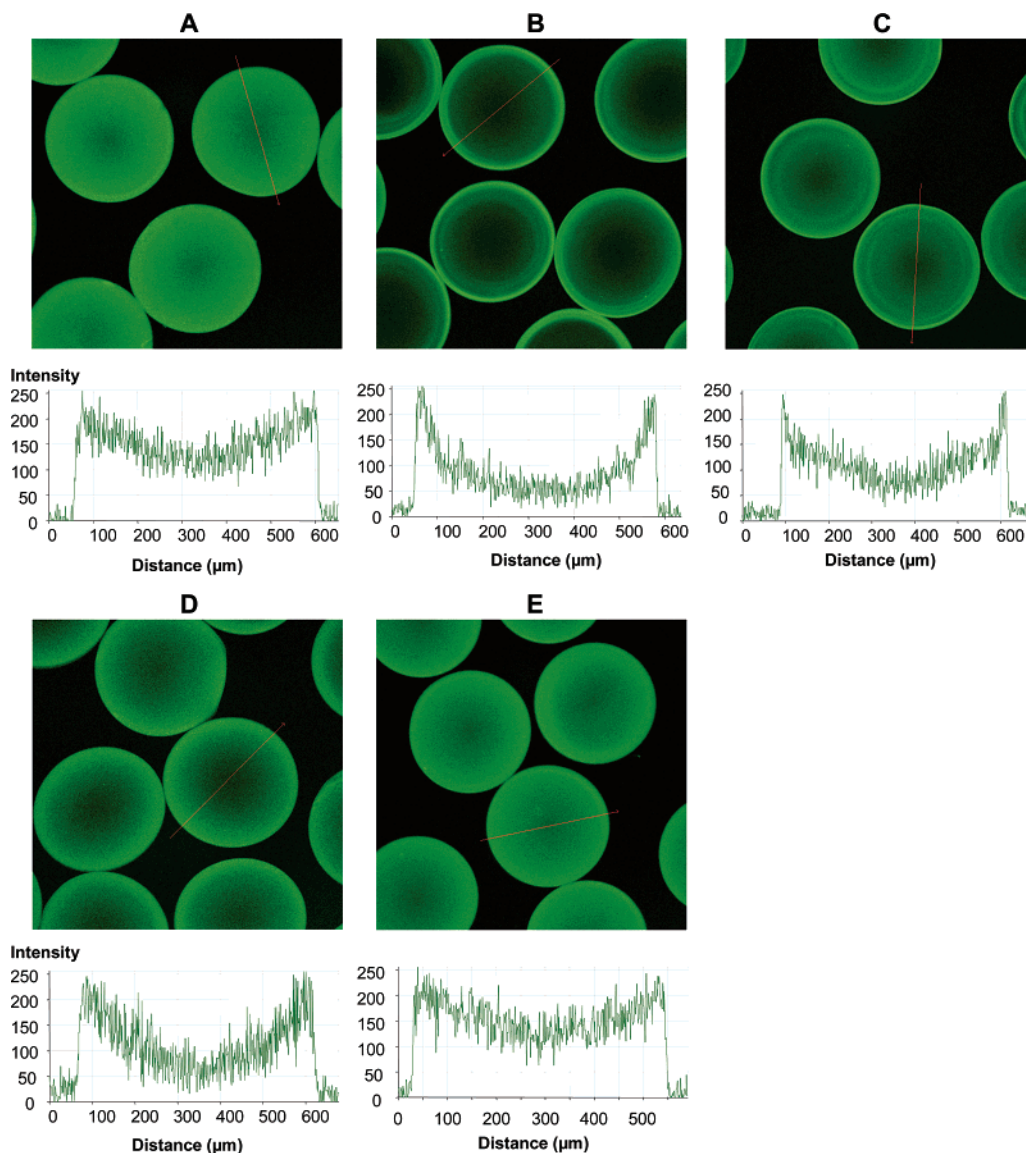


Figure 3. Alginate distribution in gel beads of fluorescence-labeled high-G alginate gelled in various gelling solutions (all in 0.15 M mannitol). A: 50 mM CaCl₂. B: 10 mM BaCl₂. C: 20 mM BaCl₂. D: 20 mM CaCl₂. E: 50 mM SrCl₂. All images are optical slices of the bead equator. Fluorescence intensity profile across the bead diameter is given below each image.

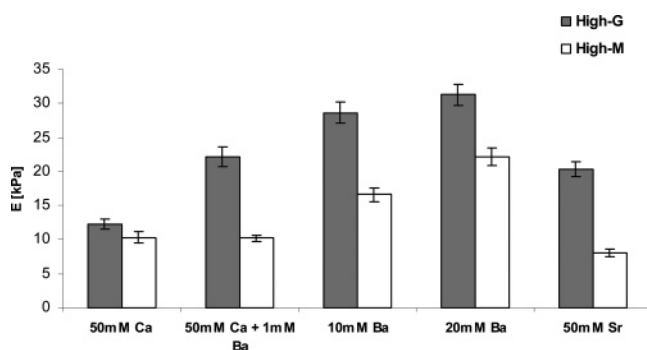


Figure 4. Gel strength (given as Young's modulus, E) for high-G and high-M alginate gel cylinders (1% (w/v)) made by internal gelling before dialysis against different solutions of barium, strontium, and calcium in 0.2 M NaCl. The values are means \pm SD of 5–7 parallels. For all gels exhibiting syneresis, the final concentration was determined and E was corrected adapting $E \propto c^2$.

in an 81% increase in the elasticity modulus. Strontium also had a positive effect on the gel strength, but to a lesser extent than Ba²⁺. This is in accordance with previous findings by Smidsrød.³² For both high-G and high-M alginate the strongest

gels were achieved when using 20 mM barium. Figure 4 further illustrates that the effect of using barium and strontium instead of calcium is not as evident for high-M alginate as it is for high-G alginate. In fact, Sr²⁺ seems to have a negative effect on the gel strength of high-M alginate gel cylinders.

Sequence–Ion-Binding Relationships of Alginates. To elucidate the discrepancy in behavior between the high-G and high-M alginates, the ion-binding properties in dilute solution were preliminarily compared at a qualitative level using circular dichroism (CD) spectroscopy. The notable modifications displayed by CD spectra of polyuronates upon treatment with junction forming ions^{33–35} are commonly allocated to the changes in the dissymmetric environment of the carboxyl chromophores ($n \rightarrow p^*$ transition) due to the proximity of the site-bound cations.^{36,37} The CD perturbation, θ (specific change in ellipticity), at each addition of junction forming divalent cation ($[\text{Polym}]_{\text{ru}}/[\text{M}^{2+}]$ ratio, R_j) can be evaluated by using eq 1

$$\theta = \left| \frac{[\theta_0] - [\theta_{R_j}]}{[\theta_0]} \right| \quad (1)$$

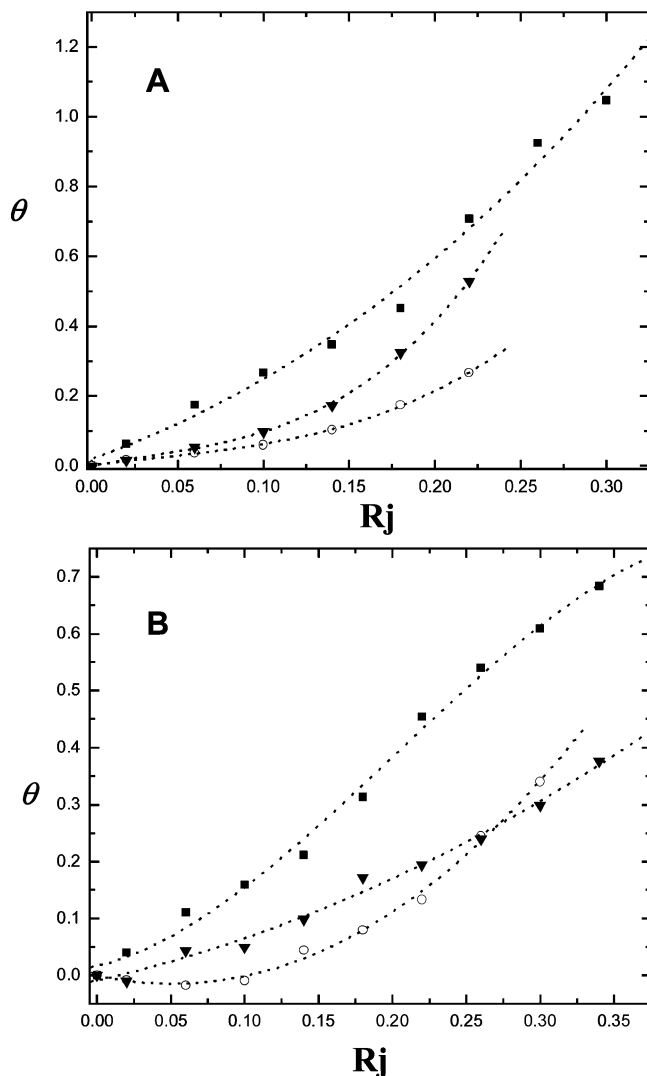


Figure 5. Specific ellipticity variation, θ , of (A) high-G and (B) high-M alginate samples upon addition of \blacksquare $\text{Ca}(\text{ClO}_4)_2$, \blacktriangledown $\text{Sr}(\text{ClO}_4)_2$, and \circ $\text{Ba}(\text{ClO}_4)_2$, respectively, at different $[\text{Polym}]_r/[\text{M}^{2+}]$ (R_j) ratios. Lines are drawn to guide the eye.

where $[\theta]_0$ and $[\theta]_{R_j}$ are the molar ellipticity values, measured at λ values corresponding to the minimum of the CD spectra of the different polyuronate solutions, without divalent ions and at a specific R_j value, respectively. According to literature, a variation of this quantity should be interpreted as the evidence of a specific “bonding” between the uronate sequence and the ion.

Figure 5A,B reports the specific ellipticity change, θ , for high-G and high-M alginates upon addition of calcium, barium, or strontium ions showing that for both alginate samples the CD spectra were found to vary (albeit to a different extent). Moreover, in both cases calcium had the largest effect on θ , suggesting a high degree of ordering of the chain upon dimerization.

In our opinion, the explanation of the macroscopic behavior of the hydrogels obtained from the different alginates relies on the assessment of interaction between the different ions and the three block components of the polysaccharide. To investigate this further, three polyuronate samples mimicking separately G-, M-, and MG-blocks (referred to as polyG, polyM, and polyMG, respectively), were analyzed by CD spectroscopy (Figure 6A–C). It should be stressed that neither an evaluation of the length of junction zones nor a quantitative comparison

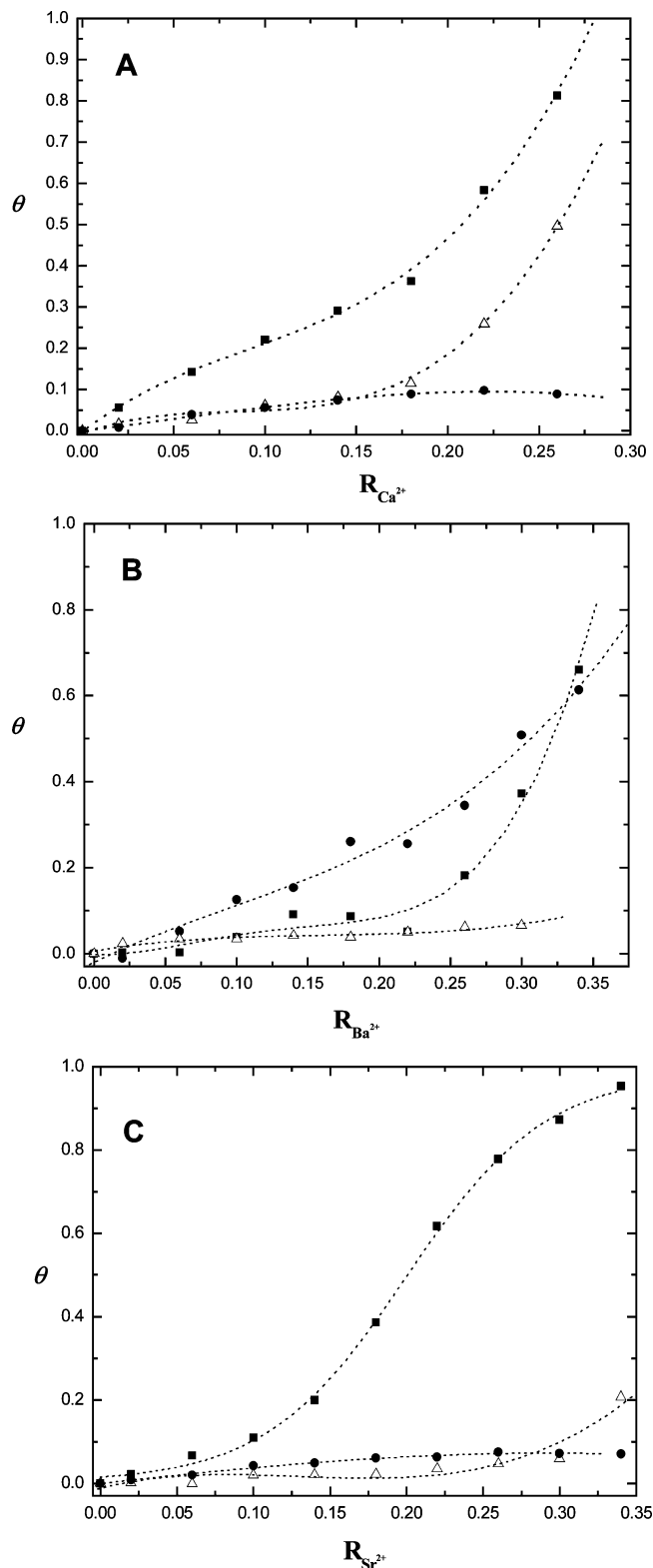


Figure 6. Specific ellipticity variation, θ , of \blacksquare polyG, \bullet polyM, and \triangle polyMG upon addition of (A) $\text{Ca}(\text{ClO}_4)_2$, (B) $\text{Ba}(\text{ClO}_4)_2$, and (C) $\text{Sr}(\text{ClO}_4)_2$ at different $[\text{Polym}]_r/[\text{M}^{2+}]$ (R_j) ratios. Lines are drawn to guide the eye.

of the ion-bonding process for the three different samples can be inferred from CD measurements alone. However, it seems feasible to conclude that variations in the specific ellipticity of the ion/polyuronate solutions stem from a strong interaction qualitatively defined as the “bonding” process.

In this sense, it might be revealing to analyze the case of calcium-treated polyM, polyG, and polyMG (Figure 6A). As

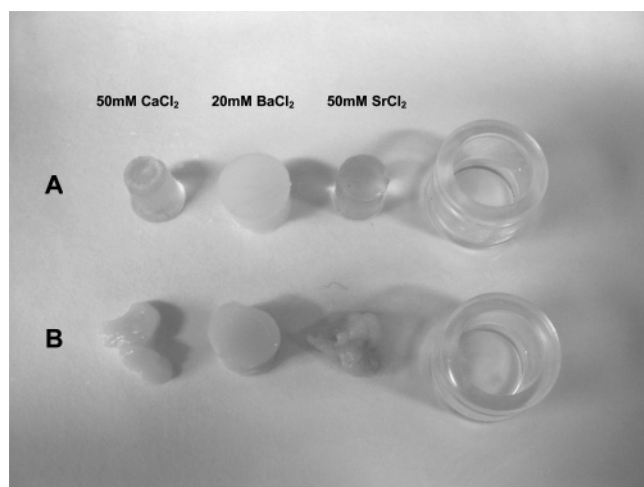


Figure 7. Alginate gel cylinders made by dialysis against different ionic solutions. A: Gels of polyMG. B: Gels of polyM. From left: Gel from 50 mM CaCl_2 , 20 mM BaCl_2 , and 50 mM SrCl_2 (all in 0.2 M NaCl). The cylinders on the right are included to show the degree of shrinkage of the gels. PolyG was not employed due to low molecular weight of the sample.

previously reported, both GG and MG sequences can efficiently coordinate calcium ions leading eventually to hydrogel formation.³⁸ Comparison between the specific ellipticity variations seems to suggest a predictably higher calcium bonding ability by G-blocks with respect to alternating sequences. On the contrary, no ion-induced chain association is detected upon treatment of mannuronan with calcium (Figure 6A).

The effect of barium on the three different uronates (Figure 6B) should hence be qualitatively analyzed along the same line. In particular, it can be pointed out that polyMG sequences do not show any specific ellipticity variation upon treatment with barium ions, while both polyG and polyM are characterized by a notable “bonding” process. Finally, in the case of Sr^{2+} , ion bonding was noted predominantly for the G sequences (i.e., polyG) (Figure 6C).

The binding of the different ions to polyM and polyMG was further investigated by forming gel cylinders by means of dialysis against calcium, barium, and strontium (polyG was not tested due to the low molecular weight of the sample). A photograph of the resulting gels is given in Figure 7. Both calcium and strontium were able to form gels with polyMG, although the gels of calcium–alginate were stronger compared to Sr–alginate gel cylinders. Both showed a high degree of shrinkage (syneresis). The gels made with barium were on the other hand weak and milky white, showing more characteristics of a precipitation rather than a gel. The gels of polyM showed the opposite effect, where the barium–alginate gel was quite strong whereas gel cylinders of calcium and strontium were too weak to hold their own weight.

Discussion

Stability and Strength of Alginate Beads. When designing an alginate capsule without the stabilizing outer polycation layer, it is especially important that the alginate gel core is stable at physiological conditions and the swelling kept at a minimum. The present study has shown that the choice of alginate is of great importance when it comes to stability of alginate gel beads with different gelling ions. Barium and strontium had a strong beneficial effect with regard to swelling on high-G alginate capsules. As seen from Figure 1, very small amounts of barium

(1 mM) in the gelling solution were sufficient to reduce the swelling of high-G alginate capsules drastically. Interestingly, no beneficial effects on swelling were observed for the high-M alginate upon exchanging the traditional calcium ions with barium or strontium. Swelling of these beads at physiological conditions may lead to increased permeability and finally to total dissolution of the gel, leaving the encapsulated cells unprotected. It has been reported before³⁹ that alginate from *M. pyrifera* in fact has a lower affinity toward barium compared to calcium, i.e., the opposite as seen for alginates from other sources, but without further explanations of the observations.

Barium also showed an extreme effect on high-G alginate gel strength, as only 1 mM of Ba^{2+} in 50 mM Ca^{2+} increased the strength of gel cylinders to the same value as high-M cylinders of 20 mM barium. This could be of importance for bioencapsulation purposes as barium has been shown to be toxic²¹ and should hence be used at minimum concentrations. It should, however, be noted that the actual barium concentration in the gel was not measured.

Table 1 shows that the high-M and high-G alginates were of different molar masses. According to Martinsen et al.²⁸ the gel strength is independent of the molecular weight of alginate samples in the range of concentrations and intrinsic viscosity used in the present study.

Permeability. Although 1 mM of Ba^{2+} was enough to increase the stability and strength of high-G alginate beads, higher amounts of barium were required to reduce the permeability toward IgG. As seen from Figure 2, only a limited amount of IgG was able to penetrate beads of high G alginate from 20 mM Ba^{2+} . Martinsen et al.²⁸ have shown that a higher concentration of alginate will result in stronger gels. Increased concentration of alginate may also result in lower permeability. Differences in polymer distribution between gel beads of high-G alginate gelled in calcium, barium, and strontium (Figure 3) may therefore be one of the reasons for the differences in permeability. In addition, the initial inhomogeneity will be better preserved for Ba–high-G-alginate beads than for beads of Ca–high-G-alginate when the gels are transferred to a saline solution.²⁶ It is therefore likely that changes in inhomogeneity during the washing procedure before the addition of IgG is to a large extent contributing to the differences seen in permeability within the high-G alginate sample when Ca^{2+} is exchanged with Ba^{2+} . Another factor that may be contributing to the permeability is the size of the gel beads, as smaller beads will have a higher total polymer concentration. This is believed to be one reason for the apparent difference in permeability between high-M and high-G capsules. High-M alginate beads had both increased bead diameter and higher swelling potential compared to high-G alginate beads (Figures 1B and 2B and Table 2). An additional explanation for differences in permeability between beads of the two alginates and differences within the high-G alginate sample may be increased cross-link density as discussed later in this paper.

Fluorescence labeling of IgG made it possible to visualize where IgG is trapped in the alginate gel. Interestingly, the immunoglobulin was able to diffuse into the center of all beads tested, even for the least permeable alginate spheres (20 mM high-G Ba–alginate). Although differences in IgG diffusion rates were observed for the various beads tested, in an in vivo situation with a time span much longer than 24 h, this deviation is probably irrelevant. It should be stressed that permeability of fluorescence-labeled IgG only gives a qualitative image showing the location of the immunoglobulin in the beads, and thus it cannot be used to measure the actual amount of IgG

that enters the beads. The two permeability methods used in this study will therefore complement rather than replace each other.

The present study showed that high-M alginate beads made in the presence of 20 mM Ba^{2+} are almost completely permeable to IgG and that the antibody is able to diffuse into the bead center. Capsules of Ba^{2+} and high-M alginate have been used to successfully protect transplanted allo- and xenograft against rejection.^{14–18} In addition, Lanza and co-workers were able to reverse diabetes in spontaneously diabetic dogs for >175 days using uncoated Ca–alginate spheres of high permeability containing canine islets.⁴⁰ Hence, capsules impermeable to IgG may not be needed to protect transplanted islets from destruction by the host immune system. Nevertheless, as small changes in capsule chemistry may lead to changes in characteristics such as permeability, the need for protection against antibody still remains uncertain.

Although the precise cutoff of the capsule membrane needed to protect the encapsulated cells from the host still is unknown, it is of course of great importance that the beads are stable to prevent the encapsulated material to be completely exposed to the host immune system. Therefore, using viable cells, this means avoiding leakage of immunogenic degradation products in combination with stable, nonswelling alginate beads might still be the most critical points in avoiding an immune reaction. In addition, the findings of the present study showing that barium is able to bind to blocks of mannuronic acid might be beneficial for transplantation purposes. Since the blocks of mannuronic acid are the most immunostimulating parts of alginate,^{41,42} it could be beneficial to cross-link the mannuronic residues which, when not cross-linked in the gel, may be able to leak out from the alginate gel beads and stimulate the immune system.⁴³

Alginate Distribution in the Gel. The distribution of polymer in the gel beads varied greatly depending on both the concentration and type of divalent ions used for gelling purposes (Figure 3). It has been shown that low concentrations of ions in the gelling solution will give the alginate more time to diffuse to the bead surface as the driving force of ions toward the gelling zone is reduced.³⁰ The result is a considerably higher concentration of alginate at the surface compared to the center of the beads. Although the concentration of ions in the gelling solution in the present study had a great effect on polymer distribution in gel beads, the type of ion used was also of importance since beads made in the presence of 20 mM Ba^{2+} still were more inhomogeneous than the corresponding 20 mM Ca–alginate gel beads (Figure 3C,D). It is well-known that barium binds more strongly to the guluronic residues in the alginate chain³² and that the number of residues required for cross-linking to occur is lower compared to calcium.⁴³ The higher inhomogeneity observed for barium–alginate beads might therefore be a result of a stronger and more rapid interaction with barium as compared to calcium, thus leading to a higher concentration of alginate at the bead surface.

The osmotic pressure in an alginate gel is proportional to the alginate concentration, while the number of cross-links is proportional to the concentration in the second power.⁸ By increasing the alginate concentration at the surface and increasing the cross-link density using barium or strontium ions in combination with an alginate with a high G content, the stability of beads should be greatly increased.

Increased inhomogeneity in the microcapsules may be beneficial to encapsulated cells as it probably is associated with less protrusion of islets, leading to an increased protection upon transplantation.²⁹ Increased stability in the outermost layer and

less polymer in the center of the capsule may also be beneficial for cells growing inside the beads.³

Considerations on the Sequence–Ion-Binding Relationships. As reported in Table 2, the initial bead size varied depending on both alginate and gelling ion used. The ion entrapment within “egg-box” structures is accompanied by a release of a notable amount of structured water, present around both the ion and the uronate groups. The amount of water released is related to the strength of the ion–uronate interaction.⁴⁴ Thus, the reduction of the diameter of the beads reflects the strength and extent of the ion–uronate binding process.

The CD studies have further elucidated the binding properties displayed by the polyuronates mimicking the three block structures present in natural alginates (namely polyG, polyM, and polyalternating) that can be summarized as follows: (i) Ca^{2+} ions bind both to G sequences and to alternating blocks, but not to M-blocks; (ii) Sr^{2+} ions bind well to polyG and not at all to polyM, while a very limited binding is detected for polyMG; (iii) Ba^{2+} ions bind both to the M and the G blocks, apparently leaving MG sequences undisturbed (Figure 6A–C).

Using ion-exchange methods, Smidsrød³² reported that the binding strength for the auto-cooperative binding of divalent ions to the three alginate fragments is as follows:

GG-blocks: $\text{Ba} > \text{Sr} > \text{Ca} \gg \text{Mg}$; MM-blocks: $\text{Ba} > \text{Sr} \sim \text{Ca} \sim \text{Mg}$; MG-blocks: $\text{Ba} \sim \text{Sr} \sim \text{Ca} \sim \text{Mg}$. The reported binding pattern of divalent ions to G blocks and M-blocks is hence in accordance with the data achieved in the present study (Figures 6 and 7). However, there is a discrepancy in the binding of ions to the polyalternating sequences as polyMG in this and a previous study by our group³⁸ has shown to bind Ca^{2+} . Here it must be kept in mind that the “MG-fraction” used in the ion-selectivity study by Smidsrød and co-workers was the acid-soluble alginate fraction of a natural alginate. This sample was later shown by ^1H NMR⁴⁵ to contain, in addition to the MG-blocks, considerable amounts of both MM- and GG-blocks ($F_{\text{GG}} = 0.13$ and $F_{\text{MM}} = 0.27$). Hence, this sample cannot be compared directly to the polyMG sample used in the present study, which consists almost solely of regular MG-sequences (Table 1).

The two alginates used in the present study differ greatly with regard to composition (Table 1). The G residues of the high-G alginate are mostly found in long G-blocks (average number of residues in G-blocks, $N_{\text{G}>1} = 15$) whereas for the high-M alginate, the guluronic acid residues are either forming short G-blocks ($N_{\text{G}>1} = 4$) or located between M residues forming an alternating structure. These differences cannot, in our opinion, be overlooked on attempting an explanation of the different behavior displayed by the two alginates.

In particular, when considering an alginate characterized by a high content of G-blocks, i.e., the high-G alginate used in the present study, the overall properties of the sample are basically determined by the behavior of GG sequences since the contribution from the MG and/or MM sequences can be neglected. It has been reported that the minimum length of G blocks necessary for junction formation decreases with increasing affinity of ions toward the alginate chain.⁴³ Therefore, upon replacing Ca^{2+} with Ba^{2+} , a higher efficiency of ion entrapment has to be expected and the presence of shorter, but likely higher in number, junctions can be predicted. The overall outcome of the combination of these effects is (i) higher stability of barium capsules compared to calcium beads as evidenced by the lower increase of diameter displayed upon saline treatment and (ii) higher gel strength evidenced by an increased elastic modulus E measured in small deformation compression. Along the same

line, the reduction of the dimensions of the capsules detected upon exchanging calcium with barium (Table 2) reflects the well-known stronger interactions between the latter and the uronic groups leading to a higher release of structured water. In view of these considerations, high-G alginate capsules prepared in the presence of Sr^{2+} display a behavior lying between Ca^{2+} and Ba^{2+} , both for the extent of junction formation (i.e., stability and mechanical properties) and strength of ion bonding (i.e., initial bead diameter as a consequence of release of structured water). Increased number of junctions may also be the explanation for a reduction in permeability of high-G barium–alginate beads compared to high-M barium–alginate beads. Further, this may be the reason for differences in permeability seen for barium and strontium beads of high-G alginate.

When alternating and MM sequences are present in substantial amount with respect to G-blocks, as in the case of the high-M alginate sample used in the present study, their involvement in the ion-binding process cannot be neglected.³⁸ It should first be noticed that calcium beads obtained from high-M alginates are more stable to NaCl treatment than the corresponding high-G alginate beads. This effect likely stems from an involvement of MG sequences in the calcium binding process: By extensively “zipping” the latter, an extra stabilization of the bead can be expected. Moreover, the “collapse” of the alternating sequences increases the release of structured water, thus affecting the diameter of the high-M alginate bead which turns out to be smaller than that of high-G alginate beads under the same experimental conditions (i.e., 50 mM CaCl_2).

A more striking effect of the composition on the gel properties is detected for high-M alginate upon replacing calcium with barium ions. In particular, it should be noted that the specific ellipticity variations displayed by polyG and polyM (Figure 6B) are rather similar, likely stemming from a comparable binding strength toward the barium ion. Moreover, only at a relatively high $R_{\text{Ba}^{2+}}$ ratio there is a crossover between the trend exhibited by polyG and polyM. One can thus suggest that the tendency to form homopolymeric (MM-MM or GG-GG) junctions is *not* much higher than the one for heteropolymeric (MM-GG) junctions for an alginate sample characterized by a similar content of G and M blocks and treated with barium ions. However, since the estimated length of the M and G residues is 4.35 Å and 5.17 Å, respectively,^{46,47} the formation of heteropolymeric MM-GG junctions represents a nonperfect packing of polyuronate chains. This will hamper their stability toward competing ions, i.e., nongelling Na ions. The higher number of junctions formed in the case of barium-treated high-M alginate beads is therefore counterbalanced by their instability toward ion-exchange, the overall result being a negligible gain in dimensional stability as compared to calcium high-M beads (see Figure 1).

When barium is used as cross-linking ion for high-M bead preparation, an increase in the initial diameter is noticed (Table 2). Since the initial dimension of the bead is related to the amount of structured water released, it follows that a less efficient ion “bonding” in junctions occurs upon replacing Ca^{2+} with Ba^{2+} . Once more this points to the presence of a substantial amount of heteropolymeric MM-GG junctions. In fact, if solely homopolymeric GG-GG junctions were involved, a reduction in the dimension of the beads would be expected as in the high-G alginate case. A further dimensional reduction should have arisen from the formation of additional homopolymeric MM-MM junctions, paralleling the MG-MG “zipping” already reported.³⁸

The behavior of high-M alginate capsules obtained by using Sr^{2+} ions deserves an additional comment. From the ion-binding/block structure relationships revealed by the CD analysis, it can be inferred that mainly G sequences are involved in the formation of junctions. As a consequence, the high-M alginate beads obtained in the presence of Sr^{2+} are smaller than those prepared with Ba^{2+} , due to the higher release of structured water induced by the perfect pairing of polysaccharide chains in homopolymeric junctions. However, the lack of contribution to ion bonding arising from alternating- or M-blocks impairs the formation of additional junctions thus explaining the lower stability of capsules and lower Young's modulus of cylinders from Sr^{2+} -treated high-M alginate compared to high-M Ca–alginate.

Conclusions

The present study has shown that when designing alginate capsules for cell immobilization, the choice of alginate as well as the type and concentration of divalent ion is essential for capsule properties such as stability and permeability. The use of barium and strontium resulted in increased stability and strength of microbeads when a high-G alginate was used compared to high-G Ca–alginate. In addition, the permeability was highly reduced upon exchanging the traditional calcium ions with Ba^{2+} . For the high-M alginate on the other hand, a beneficial effect was neither seen on stability nor permeability when gelled in Ba^{2+} or Sr^{2+} as opposed to high-M Ca–alginate. Hence, this alginate is probably not to be preferred when choosing an appropriate polymer material for beads without an additional polycation layer.

More information about sequences and block lengths of the alginates used in the present work, together with an extended analysis encompassing other alginates with different block composition, is clearly needed to fully understand the macroscopic behavior of alginate capsules and gels. Sequencing of alginates is currently being studied at our laboratories, and the availability of mannuronan C-5 epimerases makes it possible to alter the alginate block composition; these tools are expected to provide more and new insight into the ion-binding polymer–sequences relationships (work along this line is now in progress). However, it should be stressed that the two alginates used in the present study were chosen because they are the most commonly used for encapsulation purposes, which renders them of particular importance in the biotechnological and biomedical field.

Acknowledgment. This work was supported by grant to Y.A.M. by the Norwegian Research Council. The authors would like to acknowledge Massimiliano Borgogna for running circular dichroism measurements. Professor Terje Espevik is kindly thanked for providing the monoclonal mouse anti-human TNF antibody.

References and Notes

- Hasse, C.; Bohrer, T.; Barth, P.; Stinner, B.; Cohen, R.; Cramer, H.; Zimmermann, U.; Rothmund, M. *World J. Surg.* **2000**, *24*, 1361.
- Winn, S. R.; Tresco, P. A.; Zielinski, B.; Greene, L. A.; Jaeger, C. B.; Aebischer, P. *Exp. Neurol.* **1991**, *113*, 322.
- Rokstad, A. M.; Holtan, S.; Strand, B.; Steinkjer, B.; Ryan, L.; Kulseng, B.; Skjåk-Bræk, G.; Espevik, T. *Cell Transplant.* **2002**, *11*, 313.
- Haug, A.; Larsen, B.; Smidsrød, O. *Acta Chem. Scand.* **1966**, *20*, 183.
- Smidsrød, O.; Haug, A. *Acta Chem. Scand.* **1972**, *26*, 79.
- Haug, A.; Smidsrød, O. *Acta Chem. Scand.* **1970**, *24*, 843.

- (7) Haug, A. *Acta Chem. Scand.* **1961**, *15*, 1794.
- (8) Thu, B.; Bruheim, P.; Espevik, T.; Smidsrød, O.; Soon-Shiong, P.; Skjåk-Bræk, G. *Biomaterials* **1996**, *17*, 1031.
- (9) Lim, F.; Sun, A. M. *Science* **1980**, *210*, 908.
- (10) Prokop, A.; Hunkeler, D.; DiMari, S.; Haralson, M. A.; Wang, T. G. *Adv. Polym. Sci.* **1998**, *136*, 1.
- (11) Strand, B. L.; Ryan, L.; In't Veld, P.; Kulseng, B.; Rokstad, A. M.; Skjåk-Bræk, G.; Espevik, T. *Cell Transplant.* **2001**, *10*, 263.
- (12) Strand, B. L.; Mørch, Y. A.; Syvertsen, K. R.; Espevik, T.; Skjåk-Bræk, G. *J. Biomed. Mater. Res.* **2003**, *64A*, 540.
- (13) Rokstad, A. M.; Donati, I.; Borgogna, M.; Strand, B.; Espevik, T.; Skjåk-Bræk, G. Submitted for publication.
- (14) Zekorn, T.; Horcher, A.; Siebers, U.; Schnettler, R.; Klock, G.; Hering, B.; Zimmermann, U.; Bretzel, R. G.; Federlin, K. *Acta Diabetol.* **1992**, *29*, 99.
- (15) Duvivier-Kali, V. F.; Omer, A.; Parent, R. J.; O'Neil, J. J.; Weir, G. C. *Diabetes* **2001**, *50*, 1698.
- (16) Omer, A.; Duvivier-Kali, V. F.; Trivedi, N.; Wilmot, K.; Bonner-Weir, S.; Weir, G. C. *Diabetes* **2003**, *52*, 69.
- (17) Duvivier-Kali, V. F.; Omer, A.; Lopez-Avalos, M. D.; O'Neil, J. J.; Weir, G. C. *Am. J. Transplant.* **2004**, *4*, 1991.
- (18) Schneider, S.; Feilen, P. J.; Brunnenmeier, F.; Minnemann, T.; Zimmermann, H.; Zimmermann, U.; Weber, M. M. *Diabetes* **2005**, *64*, 687.
- (19) Toso, C.; Mathe, Z.; Morel, P.; Oberholzer, J.; Bosco, D.; Sainz-Vidal, D.; Hunkeler, D.; Buhler, L. H.; Wandrey, C.; Berney, T. *Cell Transplant.* **2005**, *14*, 159.
- (20) Smidsrød, O.; Haug, A.; Lian, B. *Acta Chem. Scand.* **1972**, *26*, 71.
- (21) Zimmermann, U.; Mimietz, S.; Zimmermann, H.; Hillgartner, M.; Schneider, H.; Ludwig, J.; Hasse, C.; Haase, A.; Rothmund, M.; Fuhr, G. *Biotechniques* **2000**, *29*, 564.
- (22) Gimmestad, M.; Sletta, H.; Ertesvåg, H.; Bakkevig, K.; Jain, S.; Suh, S.; Skjåk-Bræk, G.; Ellingsen, T. E.; Ohman, D. E.; Valla, S. *J. Bacteriol.* **2003**, *185*, 3515.
- (23) Ertesvåg, H.; Doseth, B.; Larsen, B.; Skjåk-Bræk, G.; Valla, S. *J. Bacteriol.* **1994**, *176*, 2846.
- (24) Kulseng, B.; Thu, B.; Espevik, T.; Skjåk-Bræk, G. *Cell Transplant.* **1997**, *6*, 387.
- (25) Liabakk, N. B.; Nustad, K.; Espevik, T. *J. Immunol. Methods* **1990**, *134*, 253.
- (26) Strand, B. L.; Mørch, Y. A.; Espevik, T.; Skjåk-Bræk, G. *Biotechnol. Bioeng.* **2003**, *82*, 386.
- (27) Draget, K. I.; Østgaard, K.; Smidsrød, O. *Carbohydr. Polym.* **1990**, *14*, 159.
- (28) Martinsen, A.; Skjåk-Bræk, G.; Smidsrød, O. *Biotechnol. Bioeng.* **1989**, *33*, 79.
- (29) Strand, B. L.; Gåserød, O.; Kulseng, B.; Espevik, T.; Skjåk-Bræk, G. *J. Microencapsul.* **2002**, *19*, 615.
- (30) Skjåk-Bræk, G.; Grasdalen, H.; Smidsrød, O. *Carbohydr. Polym.* **1989**, *10*, 31.
- (31) Thu, B.; Gåserød, O.; Paus, D.; Mikkelsen, A.; Skjåk-Bræk, G.; Toffanin, R.; Vittur, F.; Rizzo, R. *Biopolymers* **2000**, *53*, 60.
- (32) Smidsrød, O. *J. Chem. Soc., Faraday Trans.* **1974**, *57*, 263.
- (33) Morris, E. R.; Powell, D. A.; Gidley, M. J.; Rees, D. A. *J. Mol. Biol.* **1982**, *155*, 507.
- (34) Ravanat, G.; Rinaudo, M. *Biopolymers* **1980**, *19*, 2209.
- (35) Paoletti, S.; Cesaro, A.; Delben, F.; Ciana, A. *ACS Symposium Series* **1986**, *310*, 73.
- (36) Kohn, R.; Sticzay, T. *Collect. Czech. Chem. Commun.* **1977**, *42*, 2372.
- (37) Morris, E. R.; Rees, D. A.; Thom, D. J. *J. Chem. Soc., Chem. Commun.* **1973**, *7*, 245.
- (38) Donati, I.; Holtan, S.; Mørch, Y. A.; Borgogna, M.; Dentini, M.; Skjåk-Bræk, G. *Biomacromolecules* **2005**, *6*, 1031.
- (39) Haug, A.; Smidsrød, O. *Acta Chem. Scand.* **1965**, *19*, 341.
- (40) Lanza, R. P.; Ecker, D. M.; Kuhtreiber, W. M.; Marsh, J. P.; Ringeling, J.; Chick, W. L. *J. Mol. Med.* **1999**, *77*, 206.
- (41) Otterlei, M.; Østgaard, K.; Skjåk-Bræk, G.; Smidsrød, O.; Soon-Shiong, P.; Espevik, T. *J. Immunother.* **1991**, *10*, 286.
- (42) Kulseng, B.; Skjåk-Bræk, G.; Folling, I.; Espevik, T. *Scand. J. Immunol.* **1996**, *3*, 335.
- (43) Stokke, B. T.; Smidsrød, O.; Bruheim, P.; Skjåk-Bræk, G. *Macromolecules* **1991**, *24*, 4637.
- (44) Cesaro, A.; Delben, F.; Paoletti, S. *J. Chem. Soc., Faraday Trans.* **1988**, *84*, 2573.
- (45) Grasdalen, H.; Larsen, B.; Smidsrød, O. *Carbohydr. Res.* **1979**, *68*, 23.
- (46) Paoletti, S.; Cesaro, A.; Delben, F.; Crescenzi, V.; Rizzo, R. In *Macrodomains in Polymer Solutions*; Dubin, P., Ed.; Plenum Press: New York, 1985; p 159.
- (47) Atkins, E. D. T.; Nieduszynski, I. A.; Mackie, W.; Parker, K. D.; Smolko, E. E. *Biopolymers* **1973**, *12*, 1865.

BM060010D